Journal of Catalysis 263 (2009) 56–66

Contents lists available at ScienceDirect

Journal of Catalysis

www.elsevier.com/locate/jcat

Transesterification of vegetable oils on basic large mesoporous alumina supported alkaline fluorides—Evidences of the nature of the active site and catalytic performances

Marian Verziu [a], Mihaela Florea [a], Simion Simon [b], Viorica Simon [b], Petru Filip [c], Vasile I. Parvulescu [a,*], Christopher Hardacre [d,*]

[a] University of Bucharest, Department of Chemical Technology and Catalysis, Bdul Regina Elisabeta 4-12, 030018 Bucharest, Romania
[b] Faculty of Physics, Babes-Bolyai University, 1A Kogalniceanu Street, 400084 Cluj-Napoca, Romania
[c] Costin D. Nenitzescu Institute of Organic Chemistry, P.O. Box 35-108, 060023 Bucharest, Romania
[d] School of Chemistry and Chemical Engineering/QUILL, Queen's University, Belfast, Northern Ireland BT9 5AG, UK

ARTICLE INFO

Article history:
Received 29 September 2008
Revised 12 January 2009
Accepted 25 January 2009
Available online 11 February 2009

Keywords:
KF
LiF
CsF/Al_2O_3 catalysts
Transesterification
Vegetal fatty esters
Conventional heating
Microwave
Ultrasound irradiation

ABSTRACT

KF, LiF and CsF/Al_2O_3 catalysts with different loadings from 1 to 20 wt% were prepared using aqueous solutions of the alkaline fluoride compounds by wet impregnation of basic mesoporous MSU-type alumina. The catalysts were activated under Ar at 400 °C for 2 h and monitored by *in situ* XRD measurements. The catalysts were also characterized using several techniques: N_2 adsorption/desorption isotherms at −196 °C, FTIR, DR-UV–vis, CO_2-TPD, XRD, ^{27}Al CP/MAS NMR. These characterizations led to the conclusion that the deposition of alkaline fluorides on the alumina surface generates fluoroaluminates and aluminate species. The process is definitivated at 400 °C. The fluorine in these structures is less basic than in the parent fluorides, but the oxygen becomes more basic. The catalysts were tested for the transesterification of fatty esters under different experimental conditions using conventional heating, microwave and ultrasound irradiation. Recycling experiments showed that these catalysts are stable for a limited number of cycles.

1. Introduction

The transesterification of biomass feed stocks such as vegetable oil and/or animal fat with the production of "biodiesel" is one of the routes expected to lead to "green" fuels [1–4]. The reaction requires 3 mol of methanol (or a higher alcohol) and 1 mol of triglyceride to give 3 mol of fatty acid methyl (or alkyl) ester and 1 mol of glycerol (Scheme 1). Under basic conditions exchanging glycerol with the desired alkanol occurs according to the following steps.

The "green" properties of these fuels are the consequence of the fact they are nature derived compounds that means a significant reduction in greenhouse emissions, and from their composition, fuel which is essentially free of sulfur, aromatics, metals or crude oil residues. Currently, the production of fatty acid methyl esters (FAME) in Europe is encouraged due to European legislation concerning the substitution of mineral diesel by biodiesel. In this respect, the European Union aims for 12% of the total energy output to consist of biodiesel, i.e. by renewable energy.

The transesterification reaction of fatty esters triglycerides is a relatively slow reaction that requires either strong acid or base catalysts. Different catalytic systems have been used to promote these reactions and to enable lower working temperatures. Acidic catalysts were found to be more effective for low quality oils. However, under homogeneous acid catalysis (H_2SO_4, H_3PO_4, HCl, *p*-toluenesulfuric acid, $BuSn(OH)_3$, $Al(OR)_3$ etc.) the requirement of high temperature, high molar alcohol/oil ratios, separation of the catalyst, generates serious environmental and corrosion related problems that make their use non-practical for biodiesel production [3]. Conversely, using heterogeneous acid catalysts such as pure and Cs-doped heteropolyacids as unsupported materials or impregnated on various supports, such as hydrous zirconia, silica, alumina or activated charcoal, have resulted in improved acid catalyzed reactions but need either high temperatures or high molar alcohol/oil ratios [5–8]. Fe–Zn double-metal cyanide (DMC) complexes with zeolite-like cage structures were indicated to have similar activity to most of the basic oxides. These catalysts are Lewis acidic, hydrophobic (at reaction temperatures of about 443 K) structures [9].

* Corresponding authors. Fax: +40 214100241.
E-mail address: vasile.parvulescu@g.unibuc.ro (V.I. Parvulescu).

0021-9517/$ – see front matter
doi:10.1016/j.jcat.2009.01.012

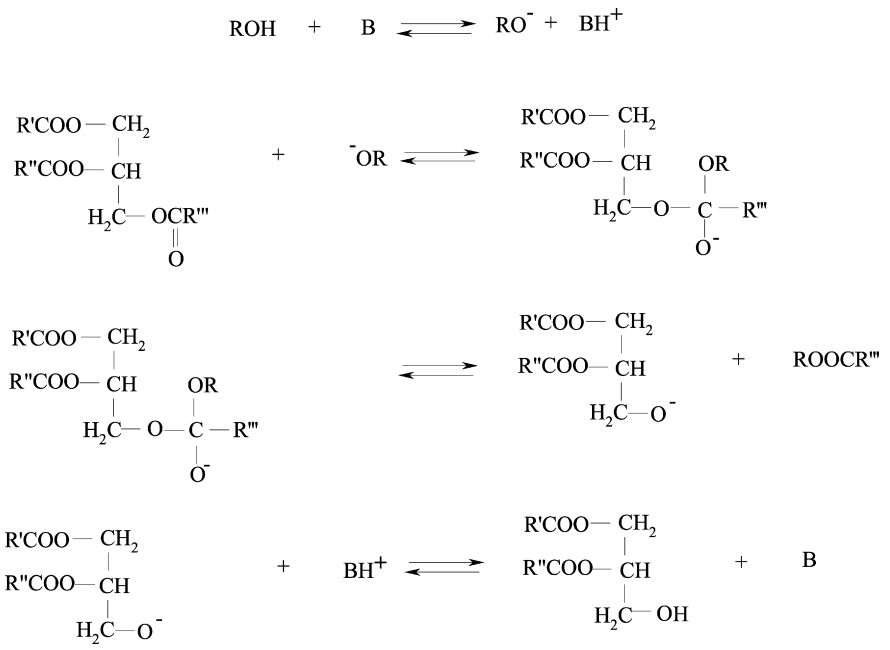

Scheme 1. Reaction pathway.

The majority of conventional produced biodiesel uses homogeneous basic catalysts such as sodium or potassium hydroxides, alkoxides, or methoxides which are very active, but present also problems of corrosion, separation and waste streams. The substitution of homogeneous catalysts with heterogeneous analogues is crucial to eliminate problems associated with homogeneous catalysts [3,10,11]. Moreover, solid catalysts can potentially be used for long periods of time allowing a technology which is capable of continuous processing thus improving the economics of biodiesel production [12]. In this scope, a large variety of solid bases have been reported including basic zeolites, metal carbonates, supported alkali metal ions and alkali earth oxides, metal oxides (PbO, PbO_2, Pb_3O_4, Tl_2O_3, and ZnO) as well as hydrotalcite derived catalysts that have been investigated in transesterification of fats to esters [12–18]. In addition, alkali nitrate and alkali carbonate-loaded Al_2O_3, polymer resins, sulfated-tin and zirconia oxides and tungstated-zirconia have also been reported [19,20]. Leaching of metal ions was encountered in the case of basic zeolite X and ETS-10 catalysts [11]. The use of these solid catalysts has, however, some drawbacks. They operate at high temperatures with high methanol–fat ratios and require protection from CO_2.

Concerning the nature of the reactor, glycerolysis of FAME has been investigated in both batch and continuous reactors [21,22]. The transesterification of fatty esters has been carried out under different activation conditions. Several studies have been reported on the production of biodiesel under microwave irradiation, using both methanol and higher alcohols. The use of this technique has the advantage of lowering oil/methanol ratio to six [23–27]. Ultrasonication was reported as well. Ultrasonication is considered to have a general accelerating effect on heterogeneous reactions. Using this technique, high biodiesel yields were shown to be achieved in a remarkably short time [28–31].

Transesterification reactions without any catalyst in near-critical or supercritical conditions using microwave irradiation have also been reported [32]. However, working under supercritical conditions requires high temperatures and pressure, resulting in higher energy consumption and the need for special equipment and safety conditions [33–37].

In this paper we report the use of various alumina supported alkaline fluoride compounds (KF/Al_2O_3, LiF/Al_2O_3 and CsF/Al_2O_3) for the transesterification of different vegetable derived fatty esters (sunflower, soybean, and rapeseed oil).

KF/Al_2O_3 is a solid base catalysts which has been extensively studied in various organic syntheses [38–49] as well as for the transesterification of palm oil with methanol to biodiesel [50]. In contrast, CsF/Al_2O_3 has only been reported for the condensation of phenols with aryl halides [51] and no reports have been found regarding the catalytic properties of LiF/Al_2O_3. However, lithium-doped ZnO and ZrO_2 catalysts were recently reported as being effective for biodiesel production [52]. Studies on using $KF–Al_2O_3$ under both microwave activation and ultrasound irradiation for different other reactions have also been examined [53–55].

Another aim of this study was to provide evidences about the nature of the active sites in this reaction. For such a purpose several techniques have been used including *in situ* XRD measurements, ^{27}Al MAS NMR, *in situ* DR-UV–vis measurements and DRIFTS.

2. Experimental

2.1. Catalysts preparation

KF, LiF and CsF/Al_2O_3 catalysts with different loadings from 1 to 30 wt% were prepared using aqueous solutions of the alkaline fluoride compounds by wet impregnation of basic mesoporous MSU-type alumina synthesized according to literature procedures [56,57]. For this purpose, in 1.65 mL, which represents the impregnation capacity of the 1.5 g support, 0.166 g (for 10 wt% MF/Al_2O_3), 0.26 g (for 15 wt% MF/Al_2O_3), 0.375 g (for 20 wt% MF/Al_2O_3) and 0.64 g (for 30 wt% MF/Al_2O_3), respectively, were dissolved. Thereafter the materials were dried overnight at room temperature and then, for 12 h at 120 °C. Before use, the catalysts were activated under Ar at 400 °C for 2 h. The activation of the catalysts was also been checked by *in situ* XRD measurements.

2.2. Catalyst characterization

The catalysts were characterized using several techniques: N_2 adsorption/desorption isotherms at −196 °C, FTIR, DR-UV–vis, CO_2-TPD, XRD, ^{27}Al CP/MAS NMR, and XPS. N_2 adsorption/desorption

Table 1
Textural characterization of the investigated catalysts.

Sample	BET surface area (m^2/g)	*t*-Plot external surface area (m^2/g)	Average pore size (Å)	Pore volume (cm^3/g)
Al_2O_3	280	262	89	0.75
10 wt% KF/Al_2O_3	236	201	107	0.70
15 wt% KF/Al_2O_3	204	171	110	0.62
20 wt% KF/Al_2O_3	179	150	89 + 125	0.55
30 wt% KF/Al_2O_3	132	107	74 + 142	0.47
10 wt% LiF/Al_2O_3	241	208	97	0.71
20 wt% LiF/Al_2O_3	174	139	92 + 119	0.54
10 wt% CsF/Al_2O_3	223	182	89	0.68
20 wt% CsF/Al_2O_3	152	134	86 + 132	0.52

isotherms at −196 °C K were recorded with a Micromeritics 2010 apparatus and were analyzed by using the Brauner–Emmet–Teller (BET) method after degassing the samples at 150 °C for 12 h. The textural characteristics of the alumina supported fluorides are given in Table 1. FTIR investigation of the catalysts was carried out with a Thermo 4700 spectrometer with the following parameters: 300 scans, 600–4000 cm^{-1} scan range at 4 cm^{-1} resolution. DR-UV–vis spectra were collected with a Thermo Electron Specord 250 spectrometer in the range 200–800 nm, using 15 scans. Temperature-programmed desorption (TPD) of carbon dioxide was performed using an Autochem 2920 apparatus. The samples were first activated at 350 °C for 1 h and subsequently cooled to 40 °C under a helium flow. The activated materials were then saturated with dry gaseous carbon dioxide (99.999%) at the same temperature. When the adsorption finished, the sample was purged with a helium flow and then the CO_2-TPD performed at a rate of 10 °C min^{-1} to 600 °C.

X-ray diffraction (XRD) patterns were obtained on a Shimadzu XRD 7000 diffractometer using a Ni filter and CuK_α radiation. Intensity was measured by scanning steps in the 2θ ranges between 0°–90° and 40°–60°.

^{27}Al MAS-NMR spectra were recorded at room temperature on MAS-NMR Avance 400 Bruker spectrometer, at 104.2 MHz, in a 9.4 T field, with 15 kHz spinning rate, using $Al(NO_3)_3$ water solution as reference. Deconvolution of the CP/MAS NMR spectra was carried out using the DMFIT program [58]. XPS spectra were recorded at room temperature using a PHI 5600ci Multi Technique Instrument. The pressure in the analysis chamber during the analysis was 1.33 mPa. Monochromatized AlK_α radiation ($h\nu = 1486.6$ eV) was used. It was generated by bombarding the Al anode with an electron gun operated with a beam current of 12 mA and acceleration voltage of 10 kV. The spectrometer energy scale was calibrated using the Au $4f_{7/2}$ peak centered at 84.0 eV. Charge correction was made with the C 1s signal of adventitious carbon (C–C or C–H bonds) located at 284.8 eV.

2.3. Catalytic tests

Typical experiments were carried out using 23 mL sunflower, soybean or rapeseed oil and 5 mL methanol (molar ratio oil:methanol of 1:4). To this system, 300 mg catalyst were added and the reaction was carried out either in a stainless steel autoclave (2 h), under microwave (between 1 and 2 h) or ultrasound irradiation (2 h). Under autoclave conditions, the stirring rate was 1200 rpm. Microwave assisted reactions were reactions carried out with a Milestone Start S system operating at 1200 W. The temperature inside the vessel (quartz reactor) was controlled using an Accufiber optical fiber thermometer system. The stirring rate inside the reactor was 350 rpm. The ultrasound experiments were carried out with an Elma Transsonic 460/H bath working at a frequency of 35 kHz. The temperature inside the reaction vessel in the case of autoclave and ultrasound assisted experiments was controlled using a thermocouple.

Analysis of the reaction products was made using a Varian ProStar 310 HPLC equipped with a C18 column with inner diameter of 4 mm and the length of 30 cm. The mobile phase was a mixture of methanol (pump A) and isopropanol:hexane in a volume ratio 5:4 (pump B), A:B of 85:15 with a flow of 0.8 mL min^{-1}. The analysis was made with a UV–vis detector working at $\lambda = 205$ nm. The identification of the products was made using a GC-MS Carlo Erba Instruments QMD 1000 equipped with a Factor Four VF-5HT column with the following characteristics: 0.32 mm × 0.1 l m × 15 m working with a temperature program at a pressure of 50.8 kPa, with He as the carrier gas. The samples were solubilized in CH_2Cl_2.

The experimental procedure to test the recyclability of the catalyst was as follows. The first run was carried out as described above. Before stopping the agitation, an aliquot was sampled and analyzed following the method described above. The agitation was then stopped and the mixture was rapidly centrifuged at 6000 rpm for 10 min. The solid was recovered and subjected to the reaction–sampling–analysis-centrifugation sequence for several successive runs. No activation–outgassing step was performed between reactions.

The leaching of fluoride was checked with an atomic absorption apparatus (Analyst 800 from Perkin–Elmer) working at $\lambda =$ 396.1 nm (typical for Al) and $\lambda = 766.5$ nm (typical for K). The samples were prepared using a typical procedure for the analysis of oils by introducing 0.5 mL sample into the digestion vessel, then adding 10 mL of nitric acid 65 wt% and 2 mL hydrogen peroxide 30 wt%. The vessel was then closed and heated in the microwave oven at 210 °C for 15 min.

3. Results and discussions

3.1. Catalyst characterization

3.1.1. Thermal analysis

Thermal analysis showed (Fig. 1) a mass loss at around 250 °C assigned to the loss of the OH groups. At this temperature the transformation of AlO(OH) into Al_2O_3 also occurs [59] as shown from the associated heat effect peak. Additionally, at around 370 °C a shoulder was observed, the intensity of which intensity increased with the loading of the alkaline fluoride. This may be assigned to the formation of a new compound, and is thought to be K_3AlF_6. The mass loss at ∼900 °C is due to the loss of this compound whilst the heat effect is also associated with the phase transformation of alumina to α-Al_2O_3. The formation and the loss of K_3AlF_6 is supported not only by the linear dependence of the mass loss on the KF content but also by the XRD patterns that indicated the disappearance of the peaks assigned to this species. Based on these results all the catalysts were activated by heating at 400 °C. Similar thermal analysis curves were obtained for LiF and CsF.

3.1.2. Textural characterization

Table 1 compiles the textural properties of the investigated catalysts. *t*-plot surface confirms the fact that MSU-type alumina is indeed a mesoporous material developing an external surface with a very high pore volume. As expected, the deposition of the alkaline fluorides led to a decrease of the surface area and the pore volume. In most of cases, the impregnation of a porous support with a 30 wt% species leads to an almost complete suppression of the surface area. However, in the present cases using the MSU-type alumina a decrease of the surface area was only about 50% after the impregnation with 30 wt% KF.

Fig. 2 shows the adsorption–desorption isotherms and the pore size distribution. While the adsorption–desorption isotherms do

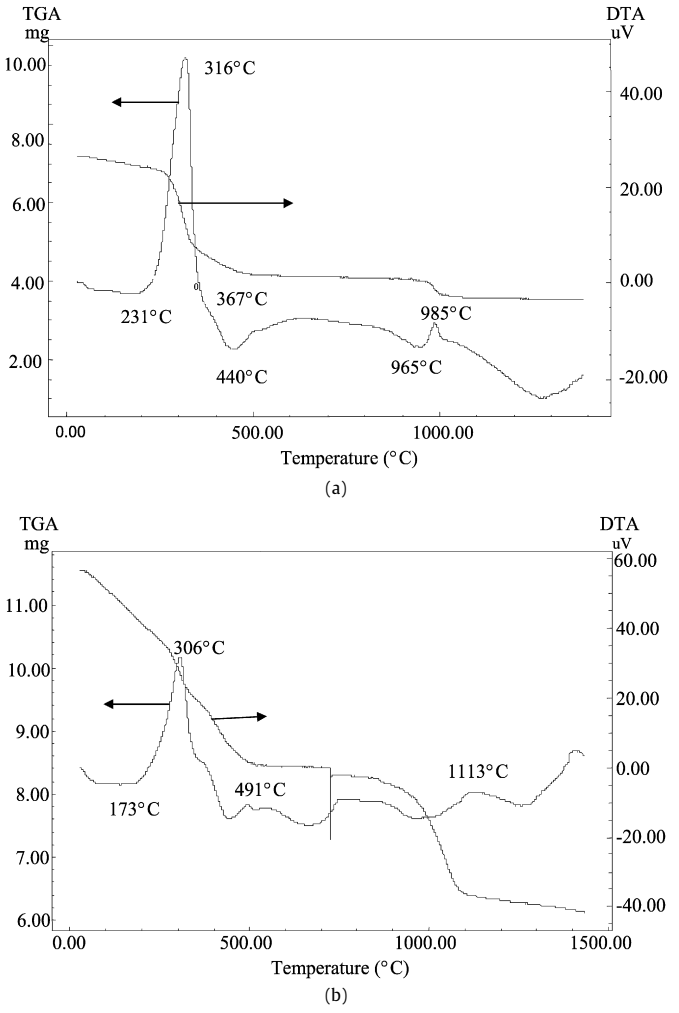

Fig. 1. TG and DTA curves for 10 wt% KF/Al_2O_3 (a) and 20 wt% KF/Al_2O_3 (b) catalysts.

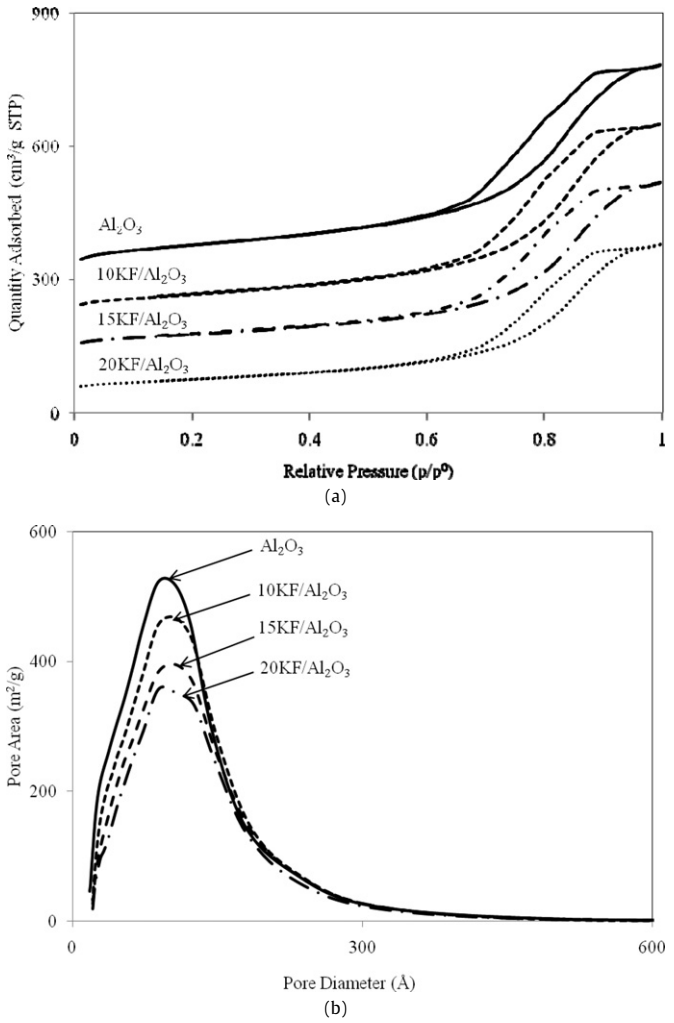

Fig. 2. Adsorption–desorption isotherms (a) and the pore size distribution (b) for KF/Al_2O_3 catalysts.

not show any important changes, except the above mentioned decrease of the pore volume, the pore size distribution shows an enlargement caused by the partial damage of the pore mouth by the deposition of the alkaline fluoride with the formation of the new compound K_3AlF_6. A bimodal distribution of the pore size has been evidenced for alkaline fluoride loadings higher than 20 wt% (Table 1).

3.1.3. XRD patterns

Fig. 3a shows the XRD patterns of the KF/Al_2O_3 catalysts and of the parent mesoporous MSU-type alumina support. These patterns confirmed that deposition of the alkaline fluoride followed by the thermal treatment led to the formation of K_3AlF_6 [60]. The intensity of the peaks assigned to this species is in agreement with the loadings of the alkaline fluoride. *In situ* XRD patterns for the 20 wt% KF/Al_2O_3 catalyst (Fig. 3b) demonstrates that the solid KF–alumina reaction starts at temperatures as low as 100 °C with the process definitivated at 400 °C. This is in a good concordance with the thermal analysis results.

3.1.4. CO_2-Thermoprogrammed desorption

Fig. 4 shows the CO_2-TPD profiles for the KF/Al_2O_3 and CsF/Al_2O_3 catalysts. They exhibit two desorption ranges. One is centered at around 100 °C and is assigned to the weak basic sites, and the second one between 400 and 500 °C is assigned to the strong basic sites. The population of the basic sites increased with the alkaline fluoride loading, and is also dependent on the alkaline species. CsF/Al_2O_3 catalysts appeared to be more basic than the KF/Al_2O_3 ones. The increase of the alkaline fluoride loadings correspond to a change of the ratios between strong and weak sites, strong sites becoming dominant. This might be a proof of the advanced reaction of the superficial alumina with the alkaline fluorides.

3.1.5. ^{27}Al CP/MAS NMR analysis

^{27}Al CP/MAS NMR analysis led to results in line with XRD measurements. The spectra given in Fig. 5 contain a symmetric line at ~10 ppm attributed to hexacoordinated aluminum in the parent mesoporous MSU-type alumina support and a line at ~0 ppm assigned to an aluminum hexacoordinated by fluorine atoms [61,62]. On increasing the KF loadings an increase was observed in both the intensity of the lines located at ~0 ppm and at ~75 ppm. The latter line has been be ascribed to tetracoordinated aluminum in $K_2Al_2O_4$ [63].

3.1.6. XPS characterization

Table 2 contains the binding energies of the $Al_{2p3/2}$, F_{1s}, $K_{2p/3/2}$, and O_{1s} levels. Fig. 6 shows the location of the $Al_{2p3/2}$ and F_{1s} levels as a function of the halide loadings. No significant change in the binding energy of the $K_{2p/3/2}$ level was found as a function of the loading of alkaline fluoride which is found to be very close to those in the parent alkaline fluoride [64]. In contrast, the binding energies of the $Al_{2p3/2}$, O_{1s} and F_{1s} levels shifted with the alkaline fluoride loading.

The binding energy of the $Al_{2p3/2}$ in the parent mesoporous MSU-type alumina support was 74.6 eV in complete agreement with previous reports [65,66]. Deposition of the alkaline fluorides led to the appearance of two more species (Fig. 6a). The binding energy of one feature occurs at around 75.0, 75.8 eV and 75.9, for LiF, KF and CsF doped materials, respectively. This component is assigned to K3AlF6 and analogous species [67,68]. The increase of the KF loadings corresponds to an increase of the population of this species; however, loadings higher that 20 wt% caused no change in the binding energy of the Al_{2p3} that may correspond to a complete superficial coverage with K_3AlF_6. A similar trend was observed for the third component located around 72.5 eV that can be assigned to aluminum in K_2AlO_4 and corresponding lithium and cesium species [69].

The deconvolution of the band assigned to the F_{1s} level indicated two components (Fig. 6b). For the system KF/Al_2O_3 the first one was located at *ca* 682.8 eV and is assigned to fluorine in a surrounding typical for the KF compound [64,70,71], while that located at 685.5 eV is assigned to fluorine in the K_3AlF_6 environment [72]. Similarly, for the systems LiF/Al_2O_3 and CsF/Al_2O_3, the first peak located at 684.4 eV and 682.1 eV, respectively, is assigned to fluorine in an environment typical for LiF and CsF [70,73], while that at 685.8 eV and 683.9 eV, respectively, to the Li_3AlF_6 and Cs_3AlF_6 environment.

From these results it is clear that, irrespective of the alkaline metal, the interaction with alumina leads to less basic fluorine than in the parent alkaline fluoride precursor. However, the charge transferred from both nitrogen and fluorine seems to be localized on oxygen that shows a second component with an increased basicity as compared with the peak contributed from the parent alumina support (Table 2). However, this oxygen should be assigned to the oxygen belonging to M_2AlO_4, resulted during the thermal treatment (Scheme 2) and also detected in XPS from the peak of the $Al_{2p3/2}$ located at cca 75.0 eV.

Previous studies dealing with KF/Al_2O_3 suggested that this system owes its basic activity due to the formation of potassium hy-

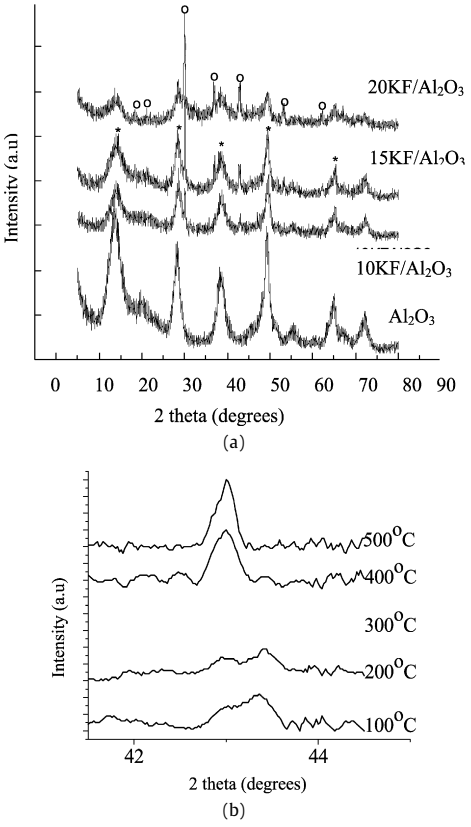

Fig. 3. XRD patterns of the calcined KF/Al_2O_3 catalysts (a) and *in situ* XRD patterns for the 20 wt% KF/Al_2O_3 catalyst in the region 2θ 42°–44° during calcining (b); (∗) AlO(OH) phase and (○) K_3AlF_6 phase.

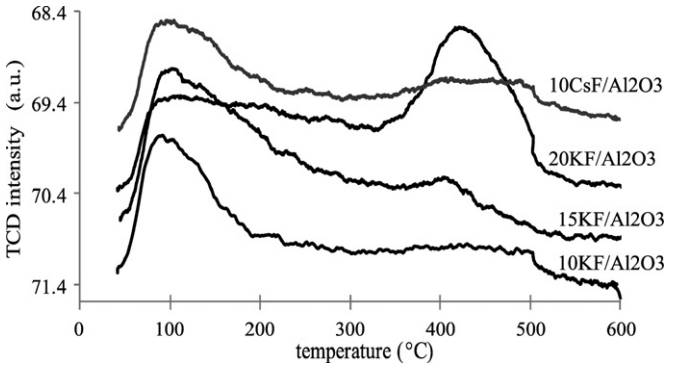

Fig. 4. The CO_2-TPD profiles for the KF/Al_2O_3 and CsF/Al_2O_3 catalysts.

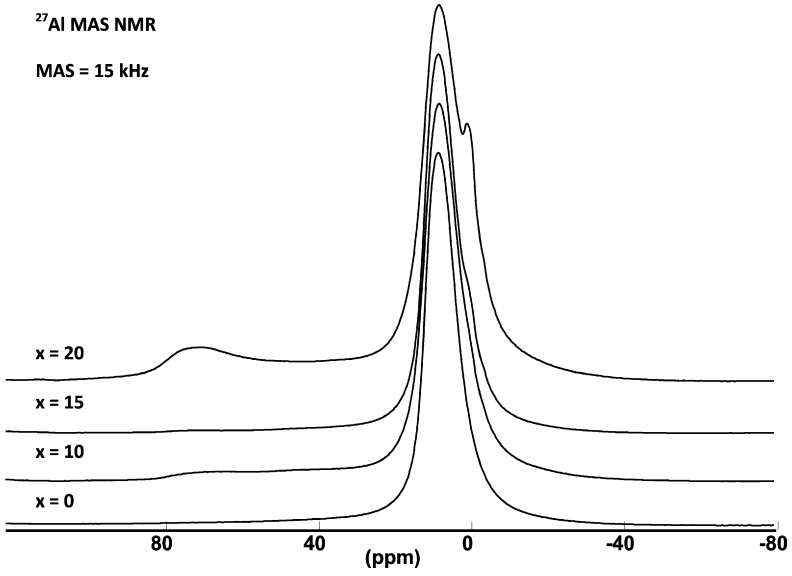

Fig. 5. ^{27}Al CP/MAS-NMR spectra of KF/Al_2O_3 catalysts.

Table 2
Binding energies of the $Al_{2p3/2}$, O_{1s}, $K_{2p/3/2}$ and F_{1s} levels.

Catalyst	Binding energy (eV)							
	$Al_{2p3/2}$			F_{1s}		$K_{2p/3/2}$	O_{1s}	
Al_2O_3		74.6		–	–	–	532.8	532.2
10 wt% KF/Al_2O_3	74.6	75.8	73.2	682.8	684.5	292.9	532.8	532.2
15 wt% KF/Al_2O_3	74.6	75.9	72.4	682.7	684.4	292.9	532.7	532.2
20 wt% KF/Al_2O_3	74.6	75.6	72.6	682.8	684.5	292.9	532.8	532.2
30 wt% KF/Al_2O_3	74.6	75.7	72.5	682.8	684.4	292.9	532.7	532.2
10 wt% LiF/Al_2O_3	74.6	75.7	72.8	684.4	685.8	292.9	532.8	532.5
20 wt% LiF/Al_2O_3	74.6	75.7	72.7	684.4	685.8	292.9	532.8	532.5
10 wt% CsF/Al_2O_3	74.6	76.2	72.8	682.1	683.9	292.9	532.7	532.0
20 wt% CsF/Al_2O_3	74.6	76.2	72.8	682.1	683.9	292.9	532.7	532.0

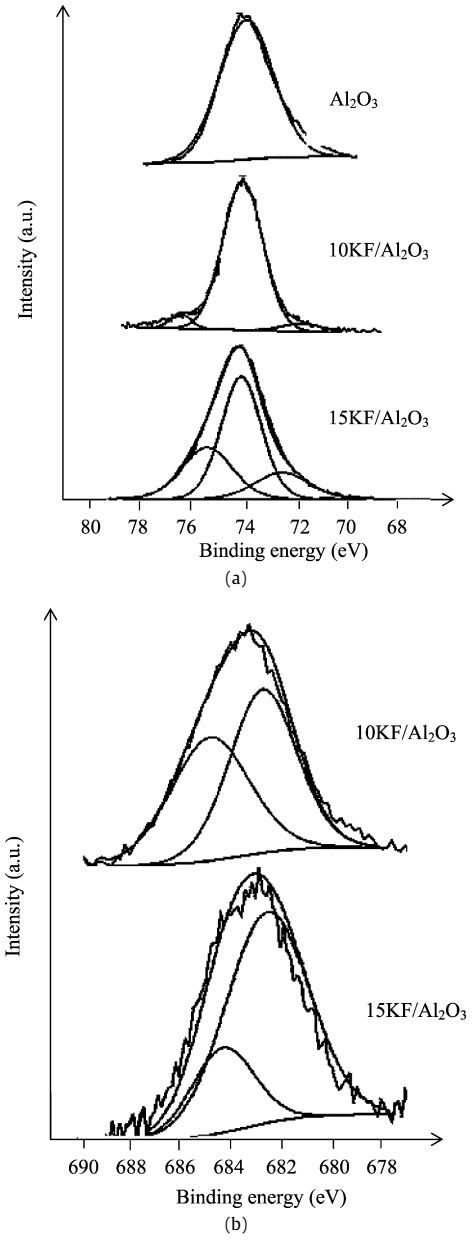

Fig. 6. XPS spectra in the region of the $Al_{2p3/2}$ (a) and F_{1s} (b) levels.

droxide and potassium hexafluoroaluminate (K_3AlF_6) during preparation [74–76]. In the present measurements no evidence for the existence of KOH was found, but the ^{27}Al NMR and XPS shows evidence which is consistent with the formation of M_2AlO_4. ^{19}F MAS NMR measurements led these authors to propose that F^- ions may be the basic sites over KF/Al_2O_3 catalysts [77,78]. However,

$$24MF + 2Al_2O_3(OH)_x \rightarrow 4M_3AlF_6 + 12MOH$$
$$12MOH + 3Al_2O_3 + 9/2O_2 \rightarrow 6M_2AlO_4 + 6H_2O$$

Scheme 2. Generation of the active sites on alumina surface.

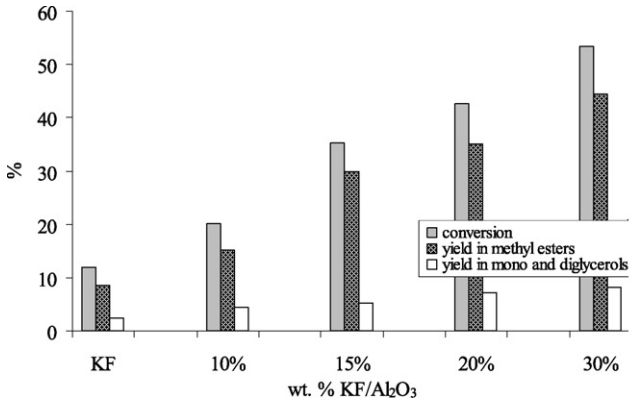

Fig. 7. Conversion and yield of the transesterification products working under conventional heating on KF/Al_2O_3 catalysts with different loadings (reaction temperature 75 °C, molar ratio methylic alcohol:sunflower oil 4:1, 2 h, stirring rate 1200 rpm, catalysts activated at 450 °C).

by comparing with pure fluorides the basicity of F^- ions in K_3AlF_6 is smaller, while the basicity of oxygen increased. Therefore, these data may lead to the idea of a cooperative effect between fluorine and oxygen leading to more basic sites than in the parent alkaline fluorides.

3.2. Catalytic transesterification

3.2.1. Sunflower oil transesterification under conventional heating

Fig. 7 shows the conversion of sunflower oil and yields to mono methyl esters and mono and diglycerols on catalysts with different loadings of KF. Both the conversion and the yields to the reaction products parallel the loading in KF. It should be noticed that no conversion of the sunflower oil was detected working with pure support. However, using pure KF under these reaction conditions the activity was almost 50% of those obtained using the supported 10 wt% KF/Al_2O_3 catalyst. Higher loadings than 30 wt% KF completely block the mesoporous pores and provide structures in which the fluoride does not interact with alumina. These data demonstrate that working with such a large mesoporous alumina support provides higher conversions and yields than working with conventional alumina [50] or metal oxide catalysts [13–15]. The methanol-to-fatty ester ratio is very close to the stoichiometric one (in this case 4) that represents further evidence of the superior activity of these catalysts as compared with conventional alumina [50] or typical metal oxides [13–15]. $KF/\gamma\text{-}Al_2O_3$ catalysts with similar KF loadings prepared according to the methodology described previously [48,49] led conversions with almost 20% smaller than the catalysts prepared in this study. Such a behavior is easy to be correlated with the much small surface area of the $KF/\gamma\text{-}Al_2O_3$ catalysts.

The activation temperature, as mentioned above, is important for the generation of active fluoroaluminate/alkaline aluminate species. TG/DTA analysis and XRD measurements indicated the formation of potassium hexafluoroaluminate is definitivated 450 °C. This matches the temperature providing the most active catalysts. Lowering the activation temperature at 350 °C corresponds to a decrease of the both conversion and yields (Fig. 8).

A significant variation in the activity was observed as a function of the alkaline fluoride used. LiF led to less active catalysts than those prepared using KF (Fig. 9), while CsF-based catalysts led to more active ones (Fig. 8). This is in line with the CO_2-TPD results that indicated CsF-based catalysts as being more basic than the KF-

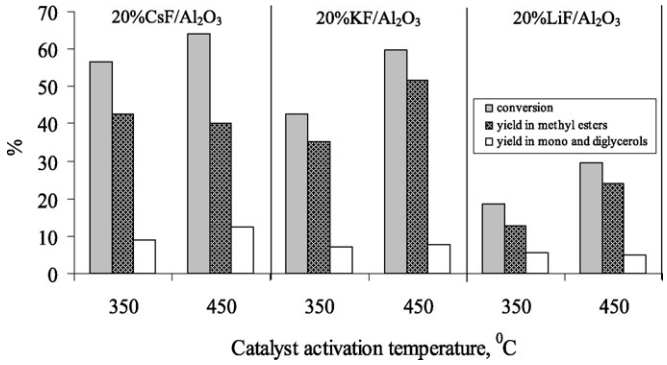

Fig. 8. Conversion and yield of the products working under conventional heating on 20 wt% alkaline fluoride/Al_2O_3 catalysts as a function of the activation temperature (reaction temperature 75 °C, 23 mL sunflower oil, molar ratio methylic alcohol:sunflower oil 4:1, 2 h, stirring rate 1200 rpm, 250 mg catalyst).

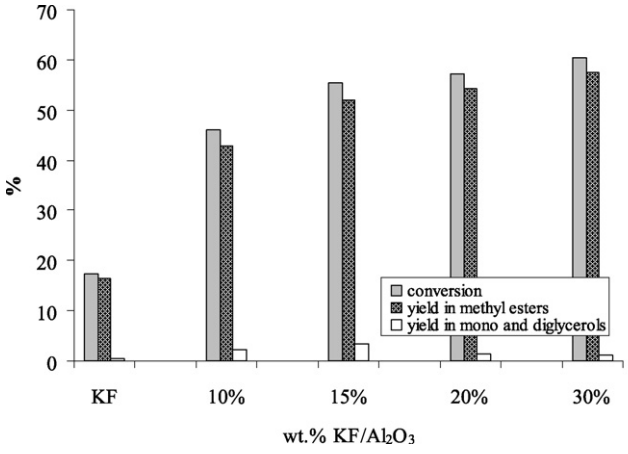

Fig. 9. Conversion and yield of the products working under microwave irradiation on KF/Al_2O_3 catalysts with different loadings (reaction temperature 72 °C, molar ratio methylic alcohol:sunflower oil 4:1, 5 min, 1200 rpm, catalysts activated at 450 °C).

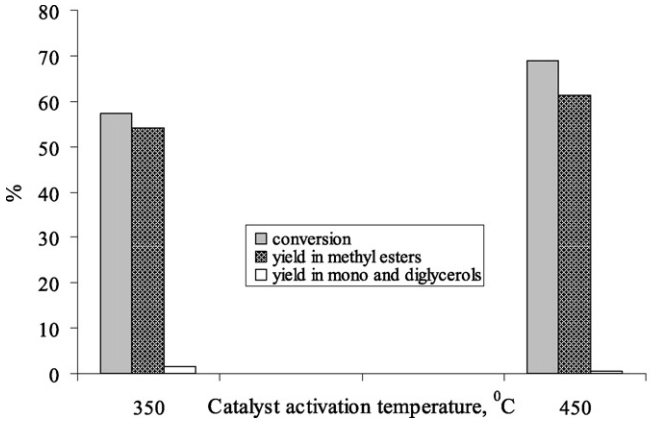

Fig. 10. Conversion and yield of the products working under microwave irradiation on 20 wt% KF/Al_2O_3 catalyst as a function of the activation temperature (23 mL sunflower oil, 5 mL methanol (molar ratio sunflower oil to methanol of 1:4), 250 mg 20 wt% KF/Al_2O_3, 5 min).

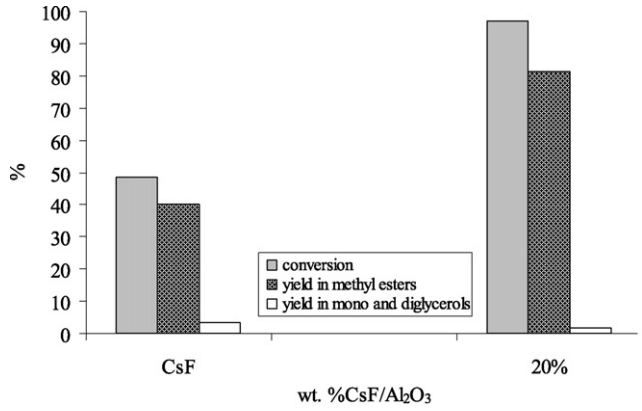

Fig. 11. Conversion and yield of the products working under microwave irradiation on CsF and 20 wt% CsF/Al_2O_3 catalyst (23 mL sunflower oil, reaction temperature 72 °C, molar ratio methylic alcohol:sunflower oil 4:1, 2 h, 1200 rpm, catalyst activated at 450 °C).

based catalysts. The activation temperature exhibit the same effect (Fig. 8).

3.2.2. Sunflower oil transesterification under microwave irradiation

Fig. 9 shows the conversion of sunflower oil and yields to mono methyl esters and mono and diglycerols on catalysts with different loadings of KF under microwave irradiation. Under reaction conditions identical with those used working in the conventional autoclave (temperature, molar ratio methylic alcohol:sunflower) both the conversion and the yields to FAME were complete. Furthermore, under microwave activation, even after 30 min both the conversion and yields were practically complete irrespective of the KF loadings. This is a very important advantage of using this technique, since these reactions do not require high loadings of the supported fluoride. Shortening the reaction time to 5 min allows the differences induced by the fluoride loading to be examined. The KF loading is found to follow the concentration of the active sites; however, it is noticeable that conversions and yields higher than 50% are still obtained despite the short reaction times.

In the early studies on microwave-assisted catalysis, the effect was interpreted as consequence of a non-thermal microwave-specific effect [79]. Detailed studies have been carried out later after that indicating that the majority of the reaction rate and product selectivity enhancements under microwave conditions can only be attributed to thermal or temperature effects which may result because of differences between the real reaction temperature at the reaction sites and the observed average temperature [79]. Many recent studies confirmed that the thermal effects observed under microwave irradiation conditions are a consequence of the inverted heat transfer, the inhomogeneities of the microwave field within the sample and the selective absorption of the radiation by polar compounds [80]. In agreement with these observations, the results presented here can be attributed to the formation of spatial hot spots at higher temperatures than the average temperatures measured using the catalyst under conventional heating.

The activation temperature has the same effect with those determined under conventional heating (Fig. 10). Samples activated at 450 °C are more active than those activated at lower temperatures.

The replacement of KF with CsF or LiF led to the same results were found under conventional heating. CsF-based catalysts led to the same performances as the KF with the same loadings but only after 1 h (Fig. 11). When one compare the TOFs, CsF-based catalysts led to almost six-times more active catalysts. However, CsF also appeared to be more active than KF. LiF-based catalysts also led to superior results compared with those obtained under conventional heating conditions (Fig. 12). However, in all cases, the LiF-based materials were found to be inferior compared with those obtained using KF- or CsF-based catalysts.

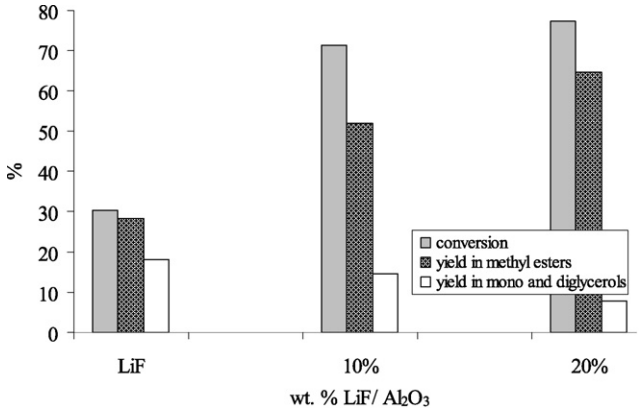

Fig. 12. Conversion and yield of the products working under microwave irradiation on LiF/Al_2O_3 supported catalysts (23 mL sunflower oil, reaction temperature 72 °C, molar ratio methylic alcohol:sunflower oil 4:1, 2 h, 1200 rpm, catalysts activated at 450 °C).

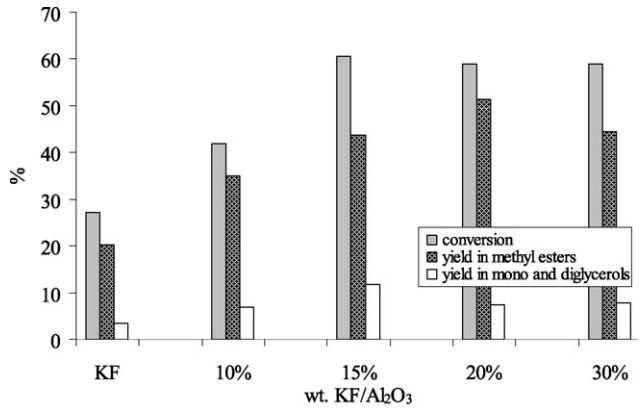

Fig. 13. Conversion and yield of the products working under ultrasound irradiation on KF/Al_2O_3 catalysts with different loadings (reaction temperature 72 °C, molar ratio methylic alcohol:sunflower oil 4:1, 2 h, catalysts activated at 450 °C).

3.2.3. Sunflower oil transesterification under ultrasound irradiation

Fig. 13 presents data on transesterification of sunflower oil under ultrasound irradiation on catalysts with different KF loadings. The results are slightly better than working under conventional heating conditions but are inferior to those obtained under microwave irradiation. As mentioned above, ultrasonication was reported to induce a general accelerating effect on heterogeneous reactions, resulting in high biodiesel yields in a remarkably short time [28–31]. In our experiments we found this partially true only compared with conventional heating. But in agreement with data reported previously [81] the major part of transesterification occurred in the first 30 min of reaction.

In contrast with the experiments carried out under conventional heating or under microwave, under ultrasound the increase of the KF loadings over 20 wt% led to a decrease in both the conversion and the yield. This behavior is due to the leaching of KF (Section 3.4). The results obtained with CsF- and LiF-based catalysts followed the same trends (Fig. 14) with CsF-based catalysts were the best performing materials and LiF-based catalysts the least active.

3.3. Transesterification of different fatty acids

Fig. 15 shows the behavior of the 20 wt% KF/Al_2O_3 catalyst in transesterification of different fatty acids under microwaves irradiation. Slight differences were observed as a function of the nature of the vegetable oil. Soybean oil was found to be more reactive than rapeseed or sunflower one. However, after 30 min

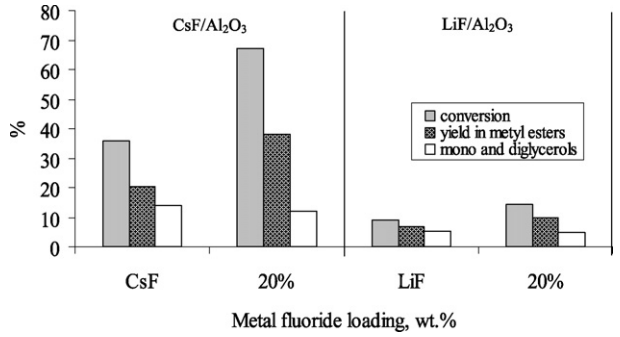

Fig. 14. Conversion and yield of the products working under ultrasound irradiation on the 20 wt% CsF/Al_2O_3 and 20 wt% LiF/Al_2O_3 catalysts (23 mL sunflower oil, reaction temperature 72 °C, 5 mL methanol (reaction temperature 72 °C, molar ratio sun flower oil to methanol of 1:4), 250 mg catalyst, activation temperature 450 °C, 2 h).

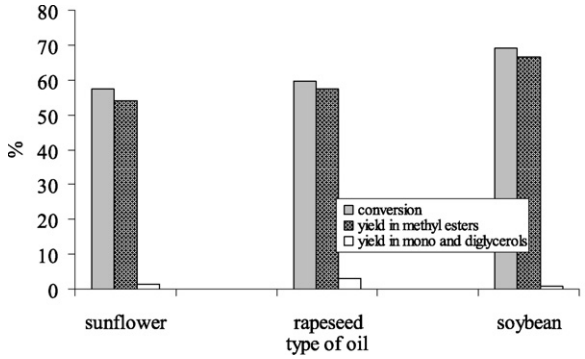

Fig. 15. Conversion and yield of the products working for different vegetable oils under microwave irradiation (23 mL vegetable oil, reaction temperature 72 °C, 5 mL methanol (molar ratio vegetable oil to methanol of 1:4), 250 mg 20 wt% KF/Al_2O_3, 5 min).

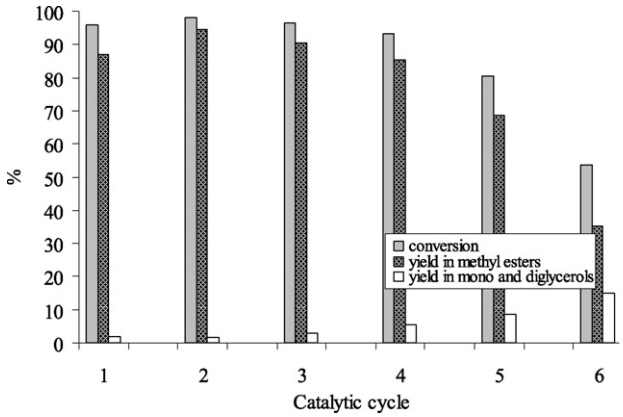

Fig. 16. Transesterification of sunflower oil under microwave conditions on 20 wt% KF/Al_2O_3 catalyst activated at 450 °C (23 mL sunflower oil, 5 mL methanol (molar ratio sunflower oil to methanol of 1:4), 250 mg 20 wt% KF/Al_2O_3, 75 °C, 2 h).

the conversion was complete for all the vegetable oils studied.

3.4. Recycling experiments and catalysts stability

The stability and recyclability of these catalysts is a very important issue. This has been checked determining the performance of the recycled catalysts without any reactivation and by chemical analysis of the FAME looking for the leached elements. Figs. 16 and 17 show the recycling experiments carried out under microwave irradiation, namely, under the most active conditions.

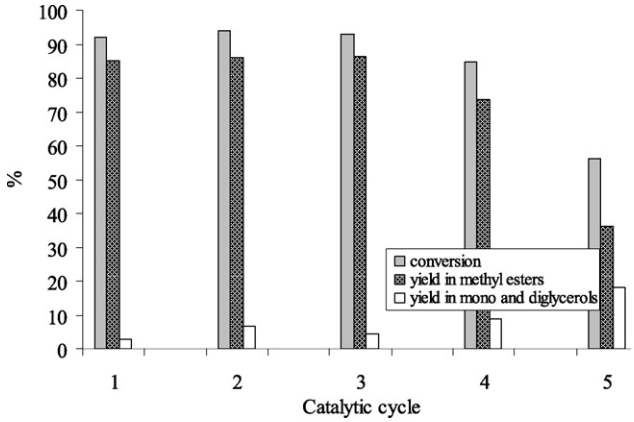

Fig. 17. Transesterification of sunflower oil under microwave conditions on 20 wt% CsF/Al_2O_3 catalyst activated at 450 °C (23 mL sunflower oil, 5 mL methanol (molar ratio sunflower oil to methanol of 1:4), 250 mg 20 wt% CsF/Al_2O_3, 75 °C, 1 h).

In the case of KF-based catalysts the conversion and the yield to the products started to decrease after forth run, while for Cs ones the deactivation was faster, namely, after the third run, although the reaction time was smaller. For the KF-based catalysts the leaching was analyzed in detail. After the first reaction, the leaching in Al and K was less than 80 ppm. However, after the fourth reaction the leaching exceed 1.5% leading to the significant drop in activity.

In order to check the effect of the reaction conditions on the leaching, both the reaction time and temperature have been reduced. Decreasing the reaction time to 5 min, led to stable catalysts for 6 and 5 runs, for KF and CsF, respectively. Also, the decrease of the reaction temperature at 30 °C was accompanied by an increase of the catalysts stability to 6 and 5 runs, respectively. These performances should be related to the smaller catalytic performances under these conditions.

The comparison of the stability of catalysts with a reduced fluoride content, namely 10 wt%, also indicated a slight improvement in the stability. The decrease in the conversion and the yield to the products started from the 6 and 5 runs, for KF and CsF, respectively, which was accompanied by values >1.2% of leached species.

3.5. General assessments

Both textural and structural characterization data and catalytic properties suggest that the properties of this system are closely related to the property of the support. MSU-type alumina is providing a highly stable surface area that made these catalysts better than the previously reported alkaline fluoride/Al_2O_3 catalysts. The characterization data confirmed the basic properties of these materials.

Corroborating data provided by the characterization techniques have been used in this study (CO_2-TPD, XRD, ^{27}Al CP/MAS NMR, and XPS) we propose the structure presented in Scheme 3 as a catalyst model. The basic site is the oxygen in the close proximity to fluorine. The basicity of fluorine is smaller than in the parent fluoride, while that of oxygen is stronger than that in the alumina support. The role of the cation is determinant in generating this basicity, cesium leading to a more basic oxygen than potassium and lithium, respectively.

In a very good concordance with this model, the transesterification of the investigated vegetable oils followed the same order CsF-based catalysts being more active than KF and LiF ones.

Typically the basicity of the alkaline fluoride/Al_2O_3 system is higher than that provided by MgO, CaO or hydrotalcites and also the stability of this catalyst is higher. By associating the higher loading of alkaline fluoride with the increased sensibility this system is generating a much better heterogeneous basic catalyst for such reactions.

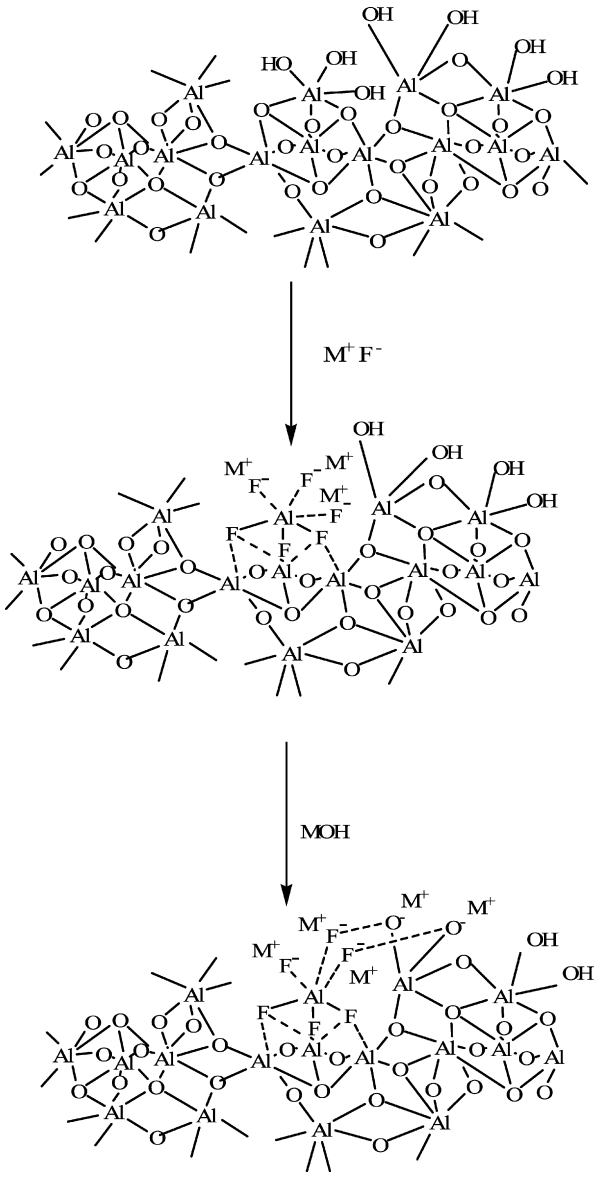

Scheme 3. The catalyst model.

It is difficult to compare results obtained at different temperatures. Therefore the results discussed in this study using conventional heating, microwave activation and ultrasound irradiation were carried out at very close temperatures in order to overcome this difficulty. Although the mechanism through which the activation is achieved using these activation procedures is different keeping close the temperature of the reaction vessel eliminates additional artifacts in interpretation of the results.

There are many examples showing that microwave irradiation is a suitable procedure to activate organic reactions carried out with heterogeneous catalysts and in the absence of a solvent. Cativiela et al. reported that in heterogeneous catalytic reactions carried out under microwave activation, only the reaction rate is changed with little change in the selectivity of the reaction observed [82]. Therein, this behavior was ascribed to the difficulty in achieving homogeneous activation by conventional heating of the catalyst due to its refractory nature while this problem can be solved by the use of microwave ovens. More recent studies [83] based on experimental and rigorous fundamental models consider that the

increase in the reaction rate is caused by a temperature rise in hot spots. This occurs in all process intensification methods which utilize a combination of microwaves and heterogeneous catalysis, irrespective of the contact time, and is directly connected with the intrinsic properties of the heterogeneous catalyst as shown by Cativiela et al. [82]. Ultrasound activation occurs via a different mechanism. Andreev [84] reported that the ultrasound irradiation increases the effectiveness of a catalyst in the form of porous granules by artificially changing the activity profile of a catalytic reaction proceeding under non-steady-state conditions. Ultrasound generates non-uniform concentration and temperature fields with time in the reaction mixture leading to activation and, in some cases, deactivation of the catalytic active center.

4. Conclusions

The deposition of alkaline fluorides on the alumina surface generates fluoroaluminates and aluminate species. The process starts at low temperatures and is definitivated at 400 °C. Fluorine in these structures is less basic than in the parent fluorides, but the oxygen becomes more basic. Therefore, the active site is thought to be the consequence of the cooperation between the fluorine and oxygen.

Using mesoporous MSU-aluminas provides large surface that allow the deposition of high loadings of alkaline fluorides. They are very active and efficient catalysts for transesterification of fatty esters with methanol at low temperatures using near stoichiometric amounts of methanol.

Recycling experiments showed that these catalysts are very stable for a limited number of cycles and do not require any intermediate activation. Leaching of the active species depends on the reaction temperature.

References

[1] T. Krawczyk, INFORM 7 (1996) 800.
[2] F. Ma, L.D. Clements, M.A. Hanna, Bioresour. Technol. 70 (1999) 1.
[3] E. Lotero, Y. Liu, D.E. Lopez, K. Suwannakarn, D.A. Bruce, J.G. Goodwin, Ind. Eng. Chem. Res. 44 (2005) 5353.
[4] M.G. Kulkarni, A.K. Dalai, Ind. Eng. Chem. Res. 45 (2006) 2913.
[5] M.G. Kulkarni, R. Gopinath, L.C. Meher, A.K. Dalai, Green Chem. 8 (2006) 1056.
[6] F. Chai, F. Cao, F. Zhai, Y. Chen, X. Wang, Z. Su, Adv. Synth. Catal. 349 (2007) 1057.
[7] K. Narasimharao, D.R. Brown, A.F. Lee, A.D. Newman, P.F. Siril, S.J. Tavener, K. Wilson, J. Catal. 248 (2007) 226.
[8] P. Morin, B. Hamad, G. Sapaly, M.G. Carneiro Rocha, P.G. Pries de Oliveira, W.A. Gonzalez, E. Andrade Sales, N. Essayem, Appl. Catal. A 330 (2007) 69.
[9] P.S. Sreeprasanth, R. Srivastava, D. Srinivas, P. Ratnasamy, Appl. Catal. A 314 (2006) 148.
[10] E. Leclercq, A. Finiels, C. Moreau, J. Am. Oil Chem. Soc. 78 (2001) 1161.
[11] G.J. Suppes, M.A. Dasari, E.J. Doskocil, P.J. Mankidy, M.J. Goff, Appl. Catal. A 257 (2004) 213.
[12] Y. Liu, E. Lotero, J.G. Goodwin Jr., X. Mo, Appl. Catal. A 331 (2007) 138.
[13] A. Corma, S. Iborra, S. Miquel, J. Primo, J. Catal. 173 (1998) 315.
[14] A.K. Singh, S.D. Fernando, Energy Fuels 22 (2008) 2067.
[15] W. Magalhaes Antunes, C. de Oliveira Veloso, C. Assumpcao Henriques, Catal. Today 133–135 (2008) 548.
[16] N. Seshu Babu, Rekha Sree, P.S. Sai Prasad, N. Lingaiah, Energy Fuels 22 (2008) 1965.
[17] T. Tittabut, W. Trakarnpruk, Ind. Eng. Chem. Res. 47 (2008) 2176.
[18] G.S. Macala, A.W. Robertson, C.L. Johnson, Z.B. Day, R.S. Lewis, M.G. White, A.V. Iretskii, P.C. Ford, Catal. Lett. 122 (2008) 205.
[19] T. Ebiura, T. Echizen, A. Ishikawa, K. Murai, T. Baba, Appl. Catal. A 283 (2005) 111.
[20] Y.M. Park, D.W. Lee, D.K. Kim, J.S. Lee, K.Y. Lee, Catal. Today 131 (2008) 238.
[21] D.S. Negi, F. Sobotka, T. Kimmel, G. Wozny, R. Schomacker, J. Am. Oil Chem. Soc. 84 (2007) 83.
[22] D.S. Negi, F. Sobotka, T. Kimmel, G. Wozny, R. Schomacker, J. Am. Oil Chem. Soc. 84 (2007) 91.
[23] T.M. Barnard, N.E. Leadbeater, M.B. Boucher, L.M. Stencel, B.A. Wilhite, Energy Fuels 21 (2007) 1777.
[24] K.M. Amore, N.E. Leadbeater, Macromol. Rapid Commun. 28 (2007) 473.
[25] C. Mazzocchia, G. Modica, A. Kaddouri, R. Nannicini, C. R. Chim. 7 (2004) 601.
[26] N.E. Leadbeater, L.M. Stencel, Energy Fuels 20 (2006) 2281.
[27] J. Hernando, P. Leton, M.P. Matia, J.L. Novella, J. Alvarez-Builla, Fuel 86 (2007) 1641.
[28] A.K. Singh, S.D. Fernando, R. Hernandez, Energy Fuels 21 (2007) 1161.
[29] K.G. Georgogianni, M.G. Kontominas, E. Tegou, D. Avlonitis, V. Gergis, Energy Fuels 21 (2007) 3023.
[30] K.G. Georgogianni, M.G. Kontominas, P.J. Pomonis, D. Avlonitis, V. Gergis, Energy Fuels 22 (2008) 2110.
[31] R.E. Armenta, M. Vinatoru, A.M. Burja, J.A. Kralovec, C.J. Barrow, J. Am. Oil Chem. Soc. 84 (2007) 1045.
[32] J. Geuens, J.M. Kremsner, B.A. Nebel, S. Schober, R.A. Dommisse, M. Mittelbach, S. Tavernier, C.O. Kappe, B.U.W. Maes, Energy Fuels 22 (2008) 643.
[33] M. Diasakou, A. Louloudi, N. Papayannakoa, Fuel 77 (1998) 1297.
[34] D. Kusdiana, S. Saka, Fuel 80 (2001) 693.
[35] G. Madras, C. Kolluru, R. Kumar, Fuel 83 (2004) 2028.
[36] W. Cao, H. Han, J. Zhang, Fuel 84 (2005) 347.
[37] R. Sawangkeaw, K. Bunyakiat, S. Ngamprasertsith, Green Chem. 9 (2007) 679.
[38] J. Muzart, J.P. Genet, A.J. Denis, Organometal. Chem. 326 (1987) C23.
[39] P. Laszlo, P. Pennetreau, Tetrahedron Lett. 26 (1985) 2645.
[40] W.J. Smith III, J.S. Sawyer, Tetrahedron Lett. 37 (1996) 299.
[41] J.H. Clark, D.J. Macquarrie, Org. Proc. Res. Dev. 1 (1997) 149.
[42] Y. Ono, T. Baba, Catal Today 38 (1997) 321.
[43] M.J. Climent, A. Corma, V. Fornes, R. Guil-Lopez, S. Iborra, Adv. Synth. Catal. 344 (2002) 1090.
[44] M. Mihara, Y. Ishino, S. Minakata, M. Komatsu, Synthesis (2003) 2317.
[45] B. Estrine, R. Soler, C. Damez, S. Bouquillon, F. Hénin, J. Muzart, Green Chem. 5 (2003) 686.
[46] B. Estrine, S. Bouquillon, F. Henin, J. Muzart, Appl. Organometal. Chem. 21 (2007) 945.
[47] Y.X. Feng, N. Yin, Q.F. Li, J.W. Wang, M.Qi. Kang, X.K. Wang, Catal. Lett. 121 (2008) 97.
[48] J.-M. Clacens, D. Genuit, B. Veldurthy, G. Bergeret, L. Delmotte, A. Garcia-Ruiz, F. Figueras, Appl. Catal. B 53 (2004) 95.
[49] B. Veldurthy, J.-M. Clacens, F. Figueras, J. Catal. 229 (2005) 237.
[50] X. Bo, X. Guomin, C. Lingfeng, W. Ruiping, G. Lijing, Energy Fuels 21 (2007) 3109.
[51] J.S. Yadav, B.V. Subba Reddy, New J. Chem. 24 (2000) 489.
[52] W. Xie, Z. Yang, H. Chun, Ind. Eng. Chem. Res. 46 (2007) 7942.
[53] H.M. Sampath Kumar, B.V. Subba Reddy, E. Jagan Reddy, J.S. Yadav, Green Chem. 1 (1999) 141.
[54] F.M. Bautista, J.M. Campelo, A. García, D. Luna, J.M. Marinas, A.A. Romero, J. Chem. Soc. Perkin Trans. 2 (2002) 227.
[55] S.-X. Wang, J.-T. Li, W.-Z. Yang, T.-S. Li, Ultrason. Sonochem. 9 (2002) 159.
[56] Z. Zhang, R.W. Hicks, T.R. Pauly, T.J. Pinnavaia, J. Am. Chem. Soc. 124 (2002) 1592.
[57] Z. Zhang, T.J. Pinnavaia, J. Am. Chem. Soc. 124 (2002) 12294.
[58] D. Massiot, F. Fayon, M. Capron, I. King, S. Le Calvé, B. Alonso, J.-O. Durand, B. Bujoli, Z. Gan, G. Hoatson, Magn. Reson. Chem. 40 (2002) 70.
[59] C.J. Brinker, G.W. Scherer, Sol–Gel Science: The Physics and Chemistry of Sol–Gel Processing, Academic Press, New York, 1990.
[60] Joint Committee on Powder Diffraction Standards, JCPDS database.
[61] S. Simon, A. van der Pol, E.J. Reijerse, A.P.M. Kentgens, G.J.M.P. van Morsel, E. de Boer, J. Chem. Soc. Faraday Trans. 91 (1995) 1519.
[62] S. Simon, G.J.M.P. van Moorsel, A.P.M. Kentgens, E. de Boer, Solid State NMR 5 (1995) 163.
[63] B.T. Poe, P.F. McMillan, B. Coté, D. Massiot, J.P. Coutures, Science 259 (1993) 786.
[64] J.J. Pireaux, N. Martensson, R. Didriksson, K. Siegbahn, J. Riga, J. Verbist, Chem. Phys. Lett. 46 (1977) 215.
[65] K. Arata, M. Hino, Appl. Catal. 59 (1990) 197.
[66] B.J. Tan, K.J. Klabunde, P.M.A. Sherwood, J. Am. Chem. Soc. 113 (1991) 855.
[67] G.E. McGuire, G.K. Schweitzer, Z.Th.A. Carlson, Inorg. Chem. 12 (1973) 2450.
[68] J. Lee, Y. Park, D.Y. Kim, J. Phys. D Appl. Phys. 35 (2002) 3171.
[69] D.E. Haycock, C.J. Nicholls, D.S. Urch, M.J. Webber, G. Wiech, J. Chem. Soc. Dalton Trans. (1978) 1785.
[70] G.E. Murch, R.J. Thorn, Phys. Chem. Solids 41 (1980) 785.
[71] Y. Kawamoto, K. Ogura, M. Shojiya, M. Takahashi, K. Kadono, J. Fluor. Chem. 96 (1999) 135.
[72] C.D. Wagner, W.M. Riggs, L.E. Davis, J.F. Moulder, G.E. Muilenberg, Handbook of X-Ray Photoelectron Spectroscopy, Perkin–Elmer Corporation, Physical Electronics Division, Eden Prairie, MI, 1979, p. 5534.
[73] W.E. Morgan, J.R. van Wazer, W.J. Stec, J. Am. Chem. Soc. 95 (1973) 751.
[74] A. Takashi, J.H. Clark, D.G. Cork, K. Takahide, Bull. Chem. Soc. Jpn. 59 (1986) 3281.
[75] L.M. Weinstock, J.M. Stevenson, S.A. Tomellini, S.H. Pan, T. Utne, R.B. Jobson, D.F. Reinhold, Tetrahedron Lett. 27 (1986) 3845.
[76] A. Takashi, J.H. Clark, D.G. Cork, H. Terukiyo, I. Junko, K. Takahide, Tetrahedron Lett. 28 (1987) 1421.
[77] T. Baba, Catal. Surv. Jpn. 4 (2000) 17.
[78] H. Handa, T. Baba, Y. Ono, J. Mol. Catal. A 134 (1998) 171.

[79] X. Zhang, D.O. Hayward, D.M.P. Mingos, Catal. Lett. 88 (2003) 33.
[80] A. de la Hoz, A. Diaz-Ortiz, A. Moreno, Chem. Soc. Rev. 34 (2005) 164.
[81] C. Stavarache, M. Vinatoru, Y. Maeda, Ultrason. Sonochem. 14 (2007) 380.
[82] C. Cativiela, J.I. García, J.A. Mayoral, E. Pires, A.J. Royo, F. Figueras, Appl. Catal. 131 (1995) 159.
[83] R. Cecilia, U. Kunz, T. Turek, Chem. Eng. Proc. 46 (2007) 870.
[84] V.V. Andreev, Ultrason. Sonochem. 6 (1999) 21.